JTTEES 7:357-373

PEER REVIEWED

Powder/Processing/Structure Relationships in WC-Co Thermal Spray Coatings: A Review of the Published Literature

H.L. de Villiers Lovelock

(Submitted 16 March 1997; in revised form 15 January 1998)

Thermally sprayed coatings based on tungsten carbide are widely used but not yet fully understood, particularly with regard to the chemical, microstructural, and phase changes that occur during spraying and their influence on properties such as wear resistance. The available literature on thermally sprayed WC-Co coatings is considerable, but it is generally difficult to synthesize all of the findings to obtain a comprehensive understanding of the subject. This is due to the many different starting powders, spray system types, spray parameters, and other variables that influence the coating structures and cause difficulties when comparing results from different workers.

The purpose of this review is to identify broad trends in the powder/processing/structure relationships of WC-Co coatings, classified according to powder type and spray method. Detailed comparisons of coating microstructures, powder phase compositions and coating phase compositions as reported by different researchers are given in tabular form and discussed. The emphasis is on the phase changes that occur during spraying. This review concerns only WC-12%Co and WC-17%Co coatings, and contrasts the coatings obtained from the cast and crushed, sintered and crushed, and agglomerated and densified powder types. Properties such as hardness, wear, or corrosion resistance are not reviewed here.

Keywords coating properties, feedstock morphology, literature survey, WC-Co coatings

1. Introduction

Tungsten carbide-cobalt (WC-Co) based materials are used extensively in industry in their sintered as well as thermally sprayed forms for applications requiring abrasion, sliding, fretting, and erosion resistance. The hard WC particles form the major wear-resistant constituent of these materials, while the cobalt binder provides toughness and support. Properties such as the hardness, wear resistance, and strength are influenced primarily by the WC grain size and volume fraction and, in the case of thermally sprayed coatings, also by varying the porosity and (often unintentionally) the carbide and binder phase composition. In the sintered material, the WC grains tend to touch one another and form a continuous "skeleton" of carbide, with the cobalt binder occupying the spaces between the carbide grains (Ref 1). In the case of thermal spray coatings, this is usually not the case, and the carbide particles tend to be more or less discrete in the matrix (Ref 2). This is due partly to the relatively high cobalt contents used (typically nominal contents of 12 and 17% compared with 6 to 10% in most sintered hard metals, Ref 1) and partly to the loss of WC or its dissolution in the cobalt matrix during thermal spraying, as is discussed in section 4 of this article.

A large number of variables affect the quality of thermal spray coatings and hence their performance in any given application. The same WC-Co coating type (e.g., "plasma sprayed WC-12%Co") can be applied using different commercial spray systems, processing parameters, and powder types. The inevitable result is a certain amount of inconsistency in the coating characteristics, even when the coatings are nominally the same.

In this literature survey, published microstructural and phase composition information for WC-Co coatings is compared to identify trends in the published powder/processing/structure relationships of the coatings. It is assumed that the reader is familiar with the characteristics of the different thermal spray processes, as well as with the microstructure of WC-Co coatings in general. Tradenames for thermal spray powders are included where available in order to facilitate identification of the exact powder used, but it should be borne in mind that the quality and/or manufacturing source of a commercial powder can be changed by the supplier.

Relatively few of the workers who have investigated WC-Co coatings supply full details of the feedstock, spray systems, and/or spray parameters used. Test conditions are often provided in broad outline only. In some cases, the percentage of cobalt in the coating is not specified. This makes detailed comparisons of results from different sources difficult. Hence, much of the coating property data summarized here serves only to identify trends. Where available, the spray system type is noted in addition to the generic terms atmospheric plasma spraying (APS), high-velocity oxyfuel combustion spraying (HVOF), and low pressure or "vacuum" plasma spraying (LPPS or VPS) for the various thermal spray processes. Important spray parameter information that is expected to have a significant effect on the coating structure is noted where it has been provided by the original source, for example "APS-ArH_2" for APS using an argon-hydrogen plasma gas mixture, and "APS-ArHe" for APS

H.L. de Villiers Lovelock, CSIR, P.O. Box 395, Pretoria, 0001, South Africa. Contact e-mail: hloveloc@csir.co.za.

with an argon-helium plasma gas mixture. In a few cases, information has been inferred from published results and is noted with an asterisk (*). For example, in cases where authors publish micrographs but have not measured coating porosity, the porosity of the coatings can be estimated from their micrographs, but the information is then subject to error.

2. Phase Equilibria in the W-C-Co System

Tungsten combines with carbon to form two hexagonally close packed (hcp) carbides, namely WC and W_2C (Fig. 1). W_2C also has other allotropic forms as can be seen in Fig. 1(b), but these are not discussed here. WC contains 6.13% C and has a microhardness of about 2400 kg/mm^2, while W_2C contains 3.16% C and has a microhardness of about 3000 kg/mm^2, but is more brittle than WC (Ref 3). Of the more commonly used metal carbides, only WC and Mo_2C have a hcp crystal structure, while most of the others (TiC, TaC, NbC, and VC) are face-centered cubic (fcc). Nevertheless the hcp WC lattice can transform to an fcc lattice by means of small atomic displacements, and hence WC and many of the other carbides are soluble in one another (Ref 3).

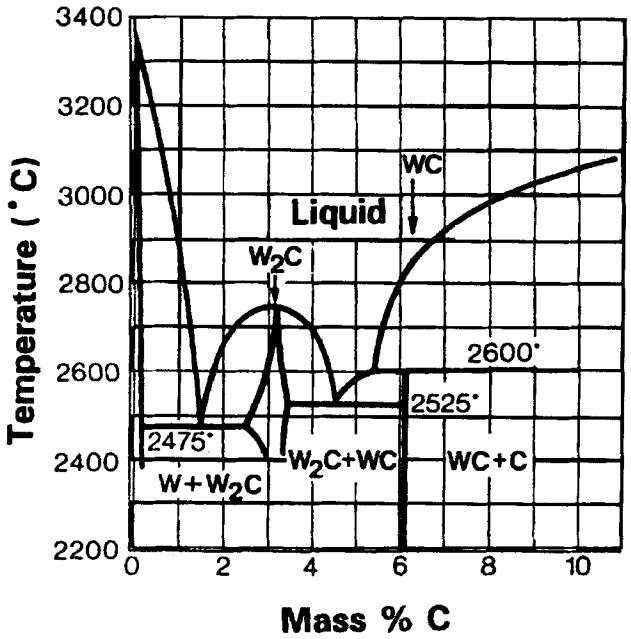

Fig. 1(a) Simplified equilibrium phase diagram for the binary system W-C, as often still quoted and used (Ref 3)

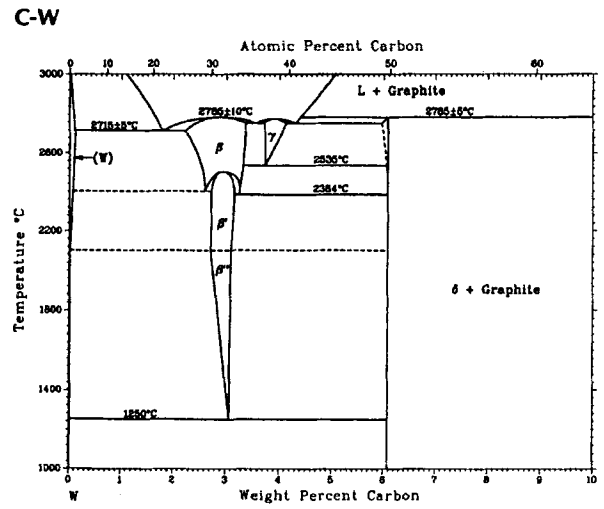

Fig. 1(b) More precise equilibrium phase diagram for the binary system W-C, taken from Baker and Okamoto (Ref 4). The three allotropic forms of W_2C are labelled β, β′, and β″, and the metastable phase γ-WC_{1-x} is shown.

The wettability of WC by most binder metals is better than that of the other carbides. This, along with its relative toughness, makes it the most widely used carbide for sintered hard metals. Cobalt is the most commonly used binder because it has excellent carbide wetting and adhesion properties. Cobalt is hcp below 700 K and fcc above that, but a significant amount of fcc phase is often retained in sintered WC-Co hard metals at room temperature (Ref 3), as well as in coatings.

Pure WC in the absence of cobalt does not melt under standard atmospheric conditions, but instead decomposes into a liquid phase and graphite above about 2780 °C, as can be seen from the phase diagram for the W-C system (Fig. 1). The ternary W-C-Co phase diagram (Fig. 2a), however, shows the existence of the brittle eta (η) phases and dissolution of WC in Co at much lower temperatures than 2780 °C. This fact is important in the HVOF thermal spray process where the flame temperature may not be high enough to decompose WC directly, but certainly could do so through the reaction of WC with the cobalt binder. The W-C-Co phase diagram is not discussed in detail here, and the reader is referred to Ref 10. It may, however, be noted that the compositional ranges of the compounds Co_3W_3C and Co_6W_6C are not fixed and also vary slightly with temperature. For example, Co_3W_3C exists in the range $Co_{3.1}W_{2.9}C$ to $Co_{2.2}W_{3.8}C$ at 1470 to 1700 K.

Despite the fact that W_2C is metastable below 1250 °C, it is often present in WC-Co, even after slow cooling (Ref 1). It is often found in commercially available powders and coatings. The metastable phase γ or WC_{1-x}, however, is only found at room temperature when the material has been quenched rapidly (Ref 11 and Fig. 1b).

Not only does WC have no stable molten phase, but it easily transforms to other embrittling phases when the carbon content is nonstoichiometric (Fig. 2). It is therefore a difficult material to successfully process in the extremely high-temperature oxidizing/decarburizing conditions generated during thermal spraying, particularly plasma spraying.

3. Coating Microstructures

3.1 Notes on Experimental Techniques Used

The cobalt binder phase of plasma sprayed WC-Co coatings often has the lamellar structure associated with such coatings, but this effect is less pronounced in HVOF sprayed coatings where the microstructure is closer to that of a sintered hard metal. The carbides are dispersed in the matrix phase, and their size is determined by the feedstock and the deposition method. Most researchers examine the coating microstructures in cross section

using optical and/or scanning electron microscopy (SEM). The microstructural parameters evaluated are usually the porosity and sometimes the size and distribution of the visibly retained carbides. Specimen preparation methods are usually not described in detail in the literature. In backscattered electron (BSE) SEM images, the larger the tungsten content, the whiter the phase appears, due to the high atomic number of tungsten (Ref 12, 13). For example, WC appears lighter than cobalt, and W_2C appears lighter than WC (Ref 14). W_2C and η phases often also have a characteristic dendritic morphology. Interference light microscopy with ZnSe films can also be used to distinguish between the different carbide phases (Ref 15). Some authors (Ref 16, 17) used Murakami's reagent to reveal the phases other than WC and cobalt in the coatings. Powders are usually examined using SEM, and both surface morphology and cross sections can be characterized.

As far as the measurement of WC sizes is concerned, none of the authors reviewed in this survey describe any specific method for quantifying the WC grain sizes in the powders or coatings, although some do mention that the powders were examined in cross section. De Villiers Lovelock, Kinds, and Young (Ref 18) used a manual graphic method applied to high magnification SEM micrographs of the powder cross sections and evaluated 100 to 120 carbide particles per powder type. The other data quoted could be estimates drawn by the relevant authors from the powder or coating cross sections, or data taken from size analysis of starting WC or WC extracted from the powders (estimated data inferred by this author from published micrographs is, as always, marked *).

3.2 Microstructures of WC-12%Co Coatings

The experimental results from the literature are summarized in Table 1(a-d) and are discussed below.

Carbide Size in Powders and Coatings. Cast and crushed powders, sintered and crushed powders, and agglomerated and densified powders and the effects on WC grain size are discussed below.

Cast and Crushed Powders. According to Jarosinski et al. (Ref 37), the cast and crushed powder examined by them contained carbides of 10 μm size. It is given by Rangaswamy and Herman (Ref 2) as 15 μm average (the corresponding micrograph contains particles ranging from about 5 to 40 μm), by Wagner et al. (Ref 38) as 1 to 20 μm, and by Mazars et al. (Ref 22) as 8 μm. Hence it appears that the carbide size in cast and crushed powders probably depends on the exact manufacturing location, but it is coarser than in the other powder types (with the exception of clad powders, which are not discussed here).

De Villiers Lovelock, Kinds, and Young (Ref 18) measured mean apparent WC sizes of between 1.7 and 3.4 μm for five cast and crushed powders representing four suppliers. Individual WC sizes of up to about 15 μm were, however, visible in some of the powder cross sections. The smaller mean WC size measured by these authors may be due to the fact that a high SEM magnification was used, revealing boundaries *within* some apparently large WC grains. These boundaries were then taken to be WC grain boundaries for the purposes of the measurement. Another reason for the discrepancy could be the measurement method—when looking at a cross section, one is more likely to see a dimension smaller than the actual diameter of the particle, because the chances that the particle is seen in cross section at its actual "equivalent" diameter are small.

Plasma sprayed coatings produced from cast and crushed powders as listed in Table 1(a) typically exhibit substantial loss or dissolution of the WC phase, or, if some WC has been retained, its average size is smaller than in the starting powder. The

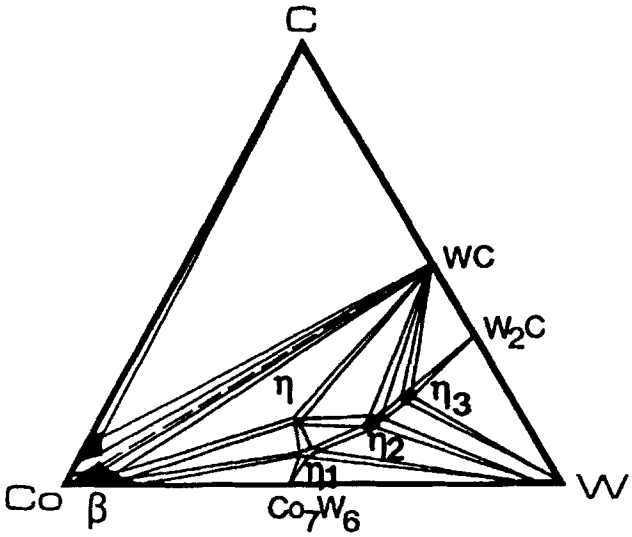

Fig. 2(a) One of the proposed equilibrium phase diagrams for the ternary system W-C-Co (section at 1400 °C). In this diagram, $\eta = M_6C$ (usually Co_3W_3C), $\eta_1 = \varepsilon$ ($M_{12}C$ or Co_6W_6C), $\eta_2 = \theta$ ($Co_3W_6C_2$) according to Rautala and Norton (Ref 6) and Barbezat et al. (Ref 7), but Co_2W_4C according to Pollock and Stadelmaier (Ref 8), and $\eta_3 = \kappa$ phase ($Co_2W_4C_4$) according to Barbezat et al. (Ref 7), but CoW_3C according to Pollock and Stadelmaier (Ref 8) and Sarin (Ref 9). The shaded areas represent the liquid phase.

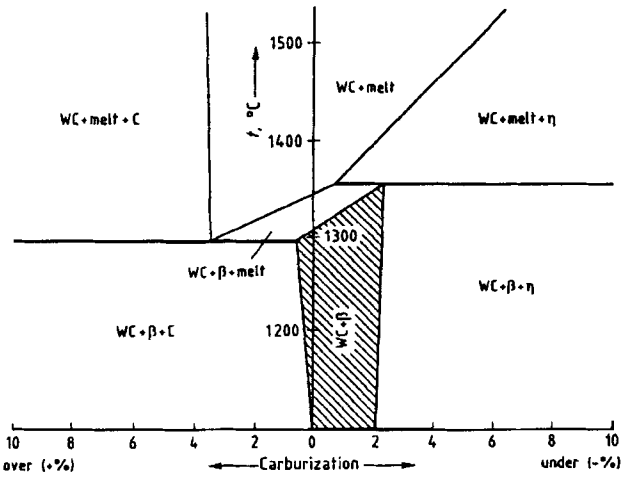

Fig. 2(b) Vertical 16 wt% Co (53 vol% Co) section from Fig. 2(a). The symbol β represents a solid solution of tungsten and carbon in cobalt, and the vertical axis represents a carbon content of 6.13 wt% (relative to the WC not to the whole alloy). Note the appearance of embrittling η (W_3Co_3C) at lower carbon contents, while the solid solution β and graphite appear together at carbon contents above 6.13%. The section shown is viewed from the cobalt corner of Fig. 2(a) and stretches perpendicularly across the line joining the cobalt and WC points in Fig. 2(a). It does not stretch across the entire width of the ternary phase diagram, hence the other ternary phases do not appear. (Redrawn from Ref 6)

HVOF coatings are listed in Table 1(b) and exhibit less WC loss than the plasma sprayed coatings, although the WC size (1 to 6 μm) is still smaller than in the original feedstock.

Sintered and Crushed Powders. According to Jarosinski et al. (Ref 37), Mazars et al. (Ref 22), Dorfman et al. (Ref 26), and Crawmer et al. (Ref 39), the sintered and crushed powders typically contain WC of 5 to 7 μm size. There seems to be less variation between suppliers compared to the cast and crushed powders. De Villiers Lovelock, Kinds, and Young (Ref 18) measured mean apparent WC sizes of between 1.0 and 1.7 μm for five sintered and crushed powder cross sections, representing four suppliers. Individual WC sizes of up to about 7 μm were, however, visible in the powder cross sections. The smaller average WC size measured by these authors may be due to the factors mentioned above for cast and crushed powders.

From Table 1(c), it can be seen that the coatings produced using sintered and crushed powder typically contain WC particles of size 1 to 2 μm (sometimes up to 4 μm). This either implies a genuine loss of carbide during spraying or the breakup of the larger apparent WC grains into the smaller ones observed by de Villiers Lovelock et al. (Ref 18). No true comparison between HVOF and plasma sprayed coatings is possible from the published results, but it would appear from Table 1(c) that, with care, it is possible to obtain plasma sprayed coatings with as much retained WC as the HVOF coatings, although the porosity will probably be higher.

Agglomerated and Densified Powders. According to Jarosinski et al. (Ref 37), the agglomerated and sintered/densified powders considered by them typically contained WC of size 3 to 5 μm, but Rangaswamy and Herman (Ref 2) give it as 1 to 2 μm,

Table 1(a) Published microstructural findings for plasma sprayed WC-12 % Co coatings (cast and crushed powders, all powders with nominally 4 % C_{total})

Process	Porosity, %	Findings (coating microstructure)	Reference
APS (ArH_2)	13	Average carbide size 2,7 μm ($\bar{s}$ = 1.6 μm), dendritic particles (typical of η-phase) observed. (WC-Co powder size ≈ 15-45 μm)	19
APS-9M (ArH_2)	4-6	Micrograph shows a very low proportion of retained carbides (powder size ≈ 5-45 μm, Metco 71 VF-NS(c))	20
APS-7M (ArHe)	High	WC in coating 3-20 μm* in size, 13% carbon loss relative to powder (powder ≈ 45-106 μm, Metco 71-NS(c), WC size in powder ≈ 5-40 μm*)	2
APS-7M (ArHe)	≤3	Optimized parameters. Homogeneous microstructure. Used both AI 1001 and Metco 71 VF-NS(c) powders	21
APS (ArHe)	ND	WC mostly retained (powder type Amperit 515(d), ≈5-45 μm, average WC size ≈ 8 μm)	22
APS (ArH_2)	ND	WC completely dissolved (powder type Amperit 515(d), ≈5-45 μm, average WC size ≈ 8 μm)	22
APS-F4	1.8	(Powder size used ≈ 5-45 μm, type AMDRY 301(c))	23
APS-9M (ArH_2)	<4	Only 2% WC visible in coating, 66% total C loss and 34% Co loss, relative to powder	24
High-energy plasma (HEP) (ArHe)	0.5-1.0	4-7% WC visible in coating, 38% C loss and ~20% Co loss relative to starting powder, WC size in coating 2-4 μm(a) and quite evenly distributed	24, 25, 26(b)
VPS (ArHe)	ND	WC well retained	22
VPS (ArH_2)	ND	WC mostly retained, not dissolved in binder; increase in H_2 in plasma increased the WC dissolution and led to formation of needlelike phases. Powder type Amperit 515(d), ≈5-45 μm, average WC size ≈ 8 μm	22

ND, not determined. (a) Dorfman et al. (Ref 26), publishing the same work, quote a WC size of both 1-2 and 2-4 μm and give an entirely different micrograph for the powder, but all the other results presented, including the coating microstructures, are identical. (b) Powder used was possibly type 71 VF-NS(c), size ≈ 5-45 μm. (c) Sulzer Metco, Westbury, NY. (d) H.C. Starck GmbH & Co., Singapore.

Table 1(b) Published microstructural findings for HVOF sprayed WC-12 % Co coatings (cast and crushed powders, all powders with nominally 4 % C_{total})

Process	Porosity, %	Findings (coating microstructure)	Reference
HVOF-Jet Kote	<0.2	Porosity higher for reducing flame(a) and higher powder feed rate. WC size 1-6 μm. The WC distribution is less regular when the fuel-to-oxygen ratio is reducing.	7
	ND	WC mostly retained, not dissolved in binder (powder type Amperit 515(c), ≈5-45 μm, average WC size ≈ 8 μm)	22
HVOF-DJ (propylene)	0.5-1.0	18-20% WC visible in coating, 38% C loss but no Co loss relative to starting powder, WC size 2-4 μm(b) and WC quite evenly distributed in coating	24, 25, 27
HVOF-JP 5000(d)	ND	Cast and crushed powder did not deposit well.	28

ND, not determined. (a) Kreye (Ref 29) and Kreye et al. (Ref 30) observed for the Jet Kote process that as the flame became more oxidizing, and also at higher fuel pressures, the degree of melting for WC-Co increased to a maximum and then slightly decreased, which correlates with these results. Arata et al. (Ref 31) also observed an increase in the WC decarburization with increased fuel pressure for a Jet Kote system. (b) Dorfman et al. (Ref 26), publishing the same work, quote a WC size of both 1-2 and 2-4 μm and give an entirely different micrograph for the powder, but all the other results presented, including the coating microstructures, are identical. (c) H.C. Starck GmbH & Co., Singapore. (d) TAFA, Inc., Concord, NH.

and it possibly varies with manufacturer. De Villiers Lovelock et al. (Ref 18) measured mean apparent WC sizes of between 1.3 and 1.8 μm for five of these powders in cross section (representing four suppliers). Individual WC sizes as large as 4 to 5 μm could, however, be observed in the powder cross sections.

From Table 1(d), it can be seen that the coatings produced using agglomerated and sintered/densified powder typically contain very fine WC particles of mean size <2.0 μm, but it is sometimes given as up to about 3 μm. There is no significant difference between plasma and HVOF sprayed coatings in this regard.

Loss of Visible Carbide Phases During Spraying. It may be noted that the percentage retention of visible carbide phases in the coatings is far less for cast and crushed powder than for sintered and crushed powder (5 to 20% versus about 70%, according to the results of Nerz et al., Ref 27). No data are available from Nerz et al. (Ref 27) for agglomerated 12% Co

Table 1(c) Published microstructural findings for WC-12 % Co coatings (sintered and crushed powders, all with nominally 5% C_{total} unless otherwise specified)

Process	Porosity, %	Findings (coating microstructure)	Reference
APS (ArH_2)	7	Average carbide size 2.6 μm ($\bar{s}$ = 1.1 μm)	19
APS (ArHe)	ND	WC mostly retained, not dissolved	22(a)
APS (ArH_2)	ND	WC partially dissolved	22
VPS (ArHe)	ND	WC mostly retained, not dissolved	22
VPS (ArH_2, low H_2)	ND	WC mostly retained, not dissolved	22
VPS (ArH_2, high H_2)	ND	WC partially dissolved, needlelike phases observed	22
High-energy plasma (HEP)	0.5-1.5	65-69% WC visible in coating(b), size 1-2 μm	27
	ND	50 vol% WC, with size 1-4 μm	32
VPS-F4	2.0	No microstructural observations supplied (Powder ≈ 11-53 μm, AMDRY 927(c))	23
HVOF-DJ (propylene)	0.5	67-72% WC visible in coating, WC size 1-2 μm	27
	ND	55 vol% WC, with size 1-4 μm	32
	0.5	55-60% WC visible in coating, WC size 1-2 μm, powder contained 4% C	27
HVOF-Jet Kote	ND	WC mostly retained, not dissolved	22
D-gun	ND	Flames that are very reducing increase porosity and free carbon in the coatings (%C not given)	33
HVOF-JP 5000(d)	<0.5	Regular WC distribution, some small Co "islands" (*)	28

ND, not determined. (a) Mazars et al. (Ref 22) used a powder size of about 5-45 μm (type Amperit 516(e)) with WC size ≈ 6 μm. (b) Visible WC content is given as 73-77% (for the same work) by Nerz et al. (Ref 25) and Dorfman et al. (Ref 26). (c) Sulzer Metco, Westbury, NY. (d) TAFA, Inc., Concord, NH. (e) H.C. Starck GmbH & Co., Singapore.

Table 1(d) Published microstructural findings for WC-12 % Co coatings (agglomerated powder types, all with nominally ~5% C_{total})

Powder	Process	Porosity, %	Findings	Reference
Agglomerated 5.2% C	APS (ArH_2)	12	Average carbide size 0.9 μm ($\bar{s}$ = 0.5 μm)	19
Not stated, probably agglomerated and sintered (compare Table 4)	APS-F4	Medium (≤8)(*)	Some unmelted particles, 1-2 μm carbides same size as in powder, carbides not uniformly distributed (Co "pools"), coating density 13.12	34
	VPS-F4	Low-medium (*)	1-2 μm carbides uniformly distributed, coating density 13.18	34
	HVOF-Jet Kote	Low (≤4) (*)	Uniformly distributed fine carbide phase, coating density 13.56	34
Agglomerated, sintered, densified	APS-F4	3.0	1.5-2.0 μm uniform carbides	35
	APS-7M (ArHe) (5.13%C)	Low (≤4)	14% carbon loss relative to powder, WC size in coating <1 μm*. (Powder size ≈ 20-63 μm, type Metco 72F(b), WC size in powder ≤ 2 μm*)	2
	APS (ArH_2) (5.44%C)	19	Average carbide size 1.5 μm ($\bar{s}$ = 0.9 μm)	19
Agglomerated and sintered	HVOF-CDS	0.7	Carbides extremely fine, much finer than the APS-F4 result of 1.5 μm	35
	HVOF-CDS	0.3	No microstructural observations supplied (Powder size ≈16-45 μm, type AMDRY 1927(a))	23
	"DGS"	1.5	No microstructural observations supplied (Powder type given as "DGS 12")	23
	D-gun	2.7	Carbides fine, but coarser than in CDS coating above, different powder manufacturer	35
	D-gun	ND	The aggl. sint. powder was coarser than the sintered and crushed one, and hence the porosity was higher using it. Flames that are very reducing increase the porosity and the free carbon in the coatings.	33
Agglomerated, sintered, densified	HVOF-Jet Kote	<2	Porosity higher for reducing flame (as previously noted) and higher powder feed rate. WC size about 0.5-3 μm	7
	HVOF-CDS	Not stated	WC size in powder and coating similar, about 0.5-2 μm, but cobalt volume fraction about 20% in powder and about 50% in coating	36

ND, not determined. (a) and (b) Sulzer Metco, Westbury, NY.

powders, but according to Rangaswamy and Herman (Ref 2) they lose the same relative amount of carbon as the cast and crushed powders. This is corroborated by the results in Table 2 for 17% Co powders, where sintered and crushed feedstock is superior to agglomerated and sintered feedstock, from the point of view of minimizing decarburization of WC.

In the case of cast and crushed powders, the amount of retained carbide is significantly better for HVOF sprayed materials than for plasma sprayed coatings, as would be expected. In the case of sintered and crushed powders, however, the difference is smaller. Based on the work of Nerz et al. (Ref 27), it appears that sintered and crushed powders may be less sensitive to process variables, which is an advantage. From the work of Mazars et al. (Ref 22, see Tables 1 and 2) it is clear that for all powders, the use of plasma gas compositions with higher thermal energy leads to observably more loss and/or dissolution of WC.

Coating Porosity. Published porosity values (Table 1) for the coatings vary widely, with values between <0.2% and 19% being reported. It is known that metallographic preparation methods and the methods of porosity measurement have an effect on results, and it is possible that these factors may have played a role in the results of Ramnath and Jayaraman (Ref 19), because their porosities were consistently much higher than all the others. Nevertheless, the reported range remains very wide, illustrating the extremes that are obtainable. Porosity seems to be lower when using sintered and crushed powder, but the data is scarce.

Table 2(a) Published microstructural findings for WC-17% Co coatings using sintered and crushed powders

Powder	Process	Porosity, %	Findings (coating microstructure)	Reference
Sintered crushed	APS (ArH_2)	ND	Dissolved/partially dissolved WC	22(a)
	APS (ArHe)	ND	WC mostly retained, not dissolved	22
	VPS (ArH_2)	ND	WC mostly retained, except in the case of the fine powder and highest plasma H_2 content, where it is partially dissolved with needlelike phases	22
	VPS (ArHe) & JetKote	ND	WC mostly retained, not dissolved. WC size in coating ± 3-9 μm(*)	22
	HVOF-DJ (propylene)	0.5	55-60% WC visible in coating, with size of about 1-2 μm	25, 27

ND, not determined. (a) These authors (Ref 22) used two size distributions of the same powder, i.e., 5-22 and 5-45 μm of type Amperit 525(b) (WC size was ≈ 4-5 μm). (b) H.C. Starck GmbH & Co., Singapore

Table 2(b) Published microstructural findings for WC-17% Co coatings using agglomerated type powders

Powder	Process	Porosity, %	Findings (coating microstructure)	Reference
Not stated, probably agglomerated and sintered	APS-F4	Low-medium (*) (~4-8)	±2 μm carbides same size as in powder, not uniformly distributed (Co "pools"), coating density 13.54	34
	VPS-F4	Low-medium (*)	±4 μm WC same size as in powder, carbides uniformly distributed	34
	HVOF-Jet Kote	Low (*) ≤4	±4 μm WC same size as in powder, uniform, smaller λ than APS coating	34
	VPS (ArHe)	4-6	55-65 vol% WC	5
	APS (ArHe)	1	50-60 vol% WC	
Agglomerated, sintered, and densified	APS/VPS-F4, HVOF-CDS and "DGS"	1.0-1.5	Evenly distributed fine carbide phase. Powders were types AMDRY 983 and 1983(c)	23
	APS-F4, HVOF-CDS, and VPS-F4	Medium to high (*), <1 for CDS	Carbide size in all coatings was 1-8 μm. Porosity not measured by Ref 40 but was <1% for CDS coatings produced in Ref 13. Powders were AMDRY 983 and 1983(c)	13, 40
	APS (ArHe) APS (ArH_2)	ND	WC mostly retained, not dissolved, or WC partially dissolved	22(a)
Agglomerated and sintered	VPS (ArHe) VPS (ArH_2)	ND	WC mostly retained, not dissolved, or WC mostly retained, increasing H_2 content of plasma gas led to WC being partially dissolved, with the formation of needlelike phases	22(a)
	APS-7M (ArHe)	Medium	23% C lost relative to powder, WC size in coating and powder ≈ 2-15 μm (*) (powder ≈ 11-45 μm, type Metco 73F NS-1(c))	2
	HEP	2.0	30-33% visible WC, size 8-10 μm	25, 27
Agglomerated, sintered, and densified	HVOF-Jet Kote	<1	Porosity higher for reducing flame and higher powder feed. WC size ≈ 2-7 μm.	7
		ND	WC mostly retained, not dissolved	22
	HVOF-CDS	<3	No details provided	12
Agglomerated and sintered	HVOF-DJ (propylene)	0.5	20-27% WC in coating(b), WC size ~4-6 μm	25, 27

ND, not determined. (a) Similar results were obtained using different powder sources (JK 7117, Deloro Stellite, Goshen, IN; AMDRY 983), with different average WC sizes. (b) Dorfman et al. (Ref 26) and Nerz et al. (Ref 25), publishing the same work, given a figure of 50-55% WC. (c) Sulzer Metco, Westbury, NY.

Barbezat et al. (Ref 7) have pointed out that inherent powder porosity is not always eliminated by spraying, particularly in HVOF processes where powder particles are usually not fully melted. Not even the impact forces can eliminate all porosity if the enclosed gas is heated and hence under pressure, and agglomerated powders contain considerable inherent porosity, as can be seen from the published micrographs of these powders (e.g., Ref 2, 7, 25, 32, 41). They have, however, also been reported to disintegrate in the spray jet to a greater extent than the other powder types, due to the acceleration forces, the melting of the cobalt and ternary phases, and the expansion of enclosed air in the particles. This particle disintegration would tend to decrease porosity (Ref 30, 42). Kreye et al. (Ref 30) found that higher-density coatings were obtained with agglomerated powders than with cast and crushed ones using the Jet Kote process, but the results were not quantitative enough to include in Table 1.

Porosity is generally higher for plasma sprayed coatings than for HVOF and D-gun coatings, as would be expected. It is consistently low (<2%) for HVOF coatings. For plasma sprayed coatings, it seems to decrease as the degree of melting (and hence the degree of WC loss by decarburization, dissolution, or reaction with the binder) increases, indicating that the optimal coating structure for plasma sprayed coatings may involve a compromise between low porosity and better retained WC particles. This is also true to a lesser extent in D-gun coatings, as noted by Vuoristo et al. (Ref 33). In Jet Kote HVOF coatings, less than 2% porosity could not be obtained by one set of workers using cast or agglomerated powders without causing the formation of η phases (Ref 30).

3.3 Microstructures of WC-17%Co Coatings

Similar trends may be observed for these coatings (Table 2) as for the 12% Co coatings (Table 1), but the scarcity of data makes specific observations difficult. One significant difference compared to 12% Co coatings is the varying and much larger WC size observed for coatings produced from agglomerated powders. Some of the agglomerated WC-17%Co powders on the market apparently have a larger WC size than the equivalent WC-12%Co powders. Dorfman et al. (Ref 26) measured it as about 10 μm, but Rangaswamy and Herman (Ref 2) and Mazars et al. (Ref 22) quote *mean* sizes of between 3 and 5 μm. De Villiers Lovelock, Kinds, and Young (Ref 18) measured mean WC sizes of between 1.4 and 4.2 μm for seven of these powders (representing four suppliers), which is larger than that measured for the 12% Co powders. Individual WC sizes of 10 to 15 μm were, however, visible in the powder cross sections. The smaller average WC size measured by these authors may be due to the factors mentioned previously.

4. Changes in Phase Composition and Carbon Content During Spraying

4.1 General Experimental Observations

Many researchers attribute variations in the properties of thermally sprayed WC-Co to the phase changes that occur in the material during spraying (e.g., Ref 7, 24, 28, 43, 44). In plasma spraying, the WC-Co powder tends to undergo a combination of decarburization, oxidation, reduction by reaction with the H_2 in the plasma gas, and dissolution/reaction between the WC and the cobalt binder metal during spraying, all resulting in the formation of hard and brittle phases (Ref 44, 45) such as W_2C, $Co_xW_yC_z$ (e.g., Co_3W_3C, Co_6W_6C, Co_2W_4C, $Co_3W_9C_4$), and even WO_3 and W. Although most authors mention the WC dissolving in the binder during spraying, Witold (Ref 46) sees the reaction during spraying as being one of the binder diffusing into the WC particles, which is probably more correct, but there is evidence for growth of W_2C from the surface of WC particles into the binder, possibly occurring after solidification of the splat (Ref 47). All of the abovementioned changes occurring in the WC-Co during spraying are collectively referred to as "decarburization" in this article, because they are usually accompanied by a decrease of up to 50% in the total carbon content, as has been seen in the previous section (Ref 24-27, 32, 44). Similar effects occur during HVOF spraying, but usually to a much lesser degree, as seen, for example, in Ref 28 and 44 where the HP/HVOF JP-5000 coating phase structure is very similar to the starting powder. This is primarily due to the lower temperatures attained in the HVOF process (Ref 44).

It is often difficult to identify the new phases in the coatings unequivocally on the basis of x-ray diffraction (XRD) alone, because their characteristic peaks are often broadened, convoluted, or shifted in position, and some of them may even be missing (Ref 11, 24, 41). However, other techniques, such as transmission electron microscopy (TEM), have confirmed their presence in coatings (e.g., Ref 11).

4.2 Reactions Occurring During the Coating Deposition Process

Li et al. (Ref 41) and Takigawa et al. (Ref 48) cite evidence that indicates that the flame enthalpy may be the primary driver for the initial decarburization reaction $WC \rightarrow W_2C$, while further decarburization to tungsten and WO_3 may require the presence of oxygen. Ghosh et al. (Ref 49), however, found that spraying in a nitrogen atmosphere inhibited the decomposition of WC to W_2C. Li et al. (Ref 41) also speculate that, if the first reaction is inhibited, for example, by choosing a lower temperature HVOF jet, then the second also will be inhibited. Conversely, the use of powders that already contain W_2C, such as most fused and crushed powders, encourages the formation of tungsten. This seems to be confirmed by experimental results (see section 4.2 and Table 3).

Detering et al. (Ref 51) have shown that both tungsten and cobalt are vaporized during plasma spraying and form part of the gas plasma. This helps to explain the fact that a net cobalt loss of up to 33 wt% (relative to the starting powder) has been reported to occur during plasma spraying (Ref 14, 24, 26, 51, 54, 55), but not during HVOF spraying (Ref 24). Nickel is similarly lost in the plasma spraying of WC-Ni and WC-Ni-Al powders (Ref 46).

The cubic phase WC_{1-x}, which is metastable below 2500 °C (see Fig. 1b), has been observed together with WC in coatings (Ref 31, 56-58), indicating the rapid cooling rates experienced by some of the particles during thermal spray deposition. Upon solidification, W-Co-C phases can crystallize from the melt (Ref 56, 58), sometimes in the form of very fine (nano) crystallites (Ref 11).

4.3 Effect of Decarburization on Coating Properties

Whether the formation of other carbide phases is beneficial or detrimental for wear resistance appears to depend on the details of the tribosystem under consideration and possibly also on the detailed coating composition and microstructure, because there are conflicting reports in the literature (Ref 51). Generally, however, it is considered detrimental (e.g., Ref 7, 24, 32, 33, 43, 44, 59, 60), although it appears that the integrity of the microstructure and the "toughness" of the coating are more important than the degree of loss of WC (Ref 11). Some HVOF coatings have been observed to perform better than sintered hard metals of comparable composition in mild hydroabrasive wear as well as three-body abrasion (dry sand rubber wheel) tests, and this has been tentatively ascribed to the stronger nanocrystalline matrix (Ref 17, 53). Other workers have found the coatings to wear at a higher rate than their sintered counterparts (e.g., Ref 61). This aspect is, however, beyond the scope of the current review.

4.4 Morphology and Identification of Phases Formed During the Spray Process

The free carbon liberated from WC during decarburization can be eliminated from the coating entirely by oxidation to CO or CO_2, or a limited amount (Ref 62) of it can remain dissolved in the cobalt matrix after solidification. Metallic tungsten (W) or W_2C may also be dissolved in the cobalt binder (Ref 2, 20) or be present on the surface of WC particles (Ref 44, 63). Karimi et al. (Ref 47) found as much as 30 to 40 at.% [W + C] in the cobalt matrix, both as a solid solution and in the form of ternary $Co_xW_yC_z$ carbides. They also claim that the addition of chromium to the cobalt matrix tended to inhibit the decarburization of WC and the formation of metallic tungsten, but this result can be disputed (Ref 64). Naylor (Ref 58) describes the matrix of APS, LPPS, and HVOF sprayed WC-12%Co coatings examined by him as "actually a W-Co-C phase in most regions." The Co/C/W/$Co_xW_yC_z$ binder in thermally sprayed WC-Co coatings is often predominantly amorphous due to rapid postspraying solidification (Ref 12, 24, 41, 62, 63, 65-67) with a grain size typically of the order of 4 to 8 nm (Ref 11, 47) or 10 to 18 nm (Ref 62, calculated value). Similar results have been obtained for WC-Ni coatings (Ref 68), demonstrating that the effect is probably not binder dependent.

The decomposition, dissolution, and decarburization of WC, not surprisingly, often commences on the surfaces of WC particles. Metallic tungsten crystallites have been observed on the surfaces of WC particles (Ref 44, 63). Karimi et al. (Ref 47) and Karimi and Verdon (Ref 53) observed a narrow band ~50 to 100 nm thick and consisting of W_2C and other unidentified phases, on the surfaces of the WC particles, and this was confirmed by Guilemay et al. (Ref 12). Nevertheless, even where this band was absent and the WC appeared to be unaltered, the binder phase in the immediate vicinity still consisted of nanocrystalline $Co_xW_yC_z$ compounds.

Evidence of partial recrystallization of the amorphous binder phase by means of nucleation of Co_3W_3C crystallites at the WC/Co interface has been documented by Verdon and Karimi et al. (Ref 11, 47). The amorphous Co-W-C binder alloy has been observed to recrystallize during heat treatment of the coating at about 900 K, or be transformed into crystalline $Co_xW_yC_z$ phases detectable by XRD, during vacuum or air heat treatment above about 1100 K (e.g., Ref 45, 63, 65, 69). The amorphous structure can also be partially recrystallized on the WC/binder boundaries by heat transfer from the impinging droplets of subsequent coating passes (Ref 53, 67).

Verdon and Karimi et al. (Ref 11, 47) found 4 to 8 at.% oxygen in the binder phase, but were unable to identify whether it was dissolved in the matrix or formed part of the oxide/oxycarbide phases.

4.5 Factors Influencing Phase Changes During the Spray Process

General. The extent of the WC transformation depends on the starting powder type (size, morphology, carbide size), the type of spray process, the amount of oxygen in the environment, and the spray parameters (Ref 34, 41, 44). For example, in plasma spraying, the higher the enthalpy of the plasma gas, the more WC decarburization and reaction with the binder phase can be expected, because more thermal energy is available to drive the process. Thus, an increase in the N_2 or H_2 flow in ArN_2 or ArH_2 plasmas, respectively, usually increases the loss of WC, while an Ar or ArHe plasma usually results in less decarburization than an ArH2 plasma (Ref 17, 24, 41, 45, 59). This is largely confirmed by the detailed data shown in Tables 3 and 4, especially when comparing results taken from the same source.

Table 3(a) Published XRD results for WC-12% Co powders (cast and crushed, all powders contained nominally 4% C)
Numbers represent relative major peak intensities and NOT percentages, except in the cases of Ref 19 and 45, where percentages were calculated

Process	WC	W_2C	W	M_6C, $M_{12}C$	Others	Reference
Powder	Major	...	...	Minor Co_3W_3C	...	19
	Major	Minor	Minor	Minor Co_3W_3C	...	12
	Major	Minor	...	Minor Co_3W_3C	$Co_3W_9C_4$, Co_2W_4C	2
	100	70	...	...	...	20
	Major	...	...	Significant	Cobalt	30
	47	32	7	Co_3W_3C = 11, others 3	...	25-27
	62	23	5	Trace Co_3W_3C	...	24
	Major	...	...	Significant: Co_3W_3C	...	7
	Major	...	...	Minor	...	22
	Major	Minor	...	Trace Co_3W_3C	$Co_3W_9C_4$	23

Table 3(b) Published XRD results for WC-12 % Co coatings (cast and crushed powders, all powders contained nominally 4 % C)
Numbers, where used, represent relative major peak intensities and NOT volume or mass percentages, except in the cases of Ref 19 and 45, where percentages were calculated.

Process	WC	W_2C	W	$M_6C, M_{12}C$	Others	Reference
APS-9M	61	100	89	...	(a)	20(b)
(ArH_2)	4	31	65	Trace Co_3W_3C	...	24
APS-F4	Major	Major	...	Trace	...	50
	Major	Major	Major	Trace Co_3W_3C	$Co_3W_9C_4$	23
APS (ArH_2)	Major	...	...	Minor/trace	...	22
	53%	15%	...	32%(c)	...	19
	Major	Minor	Minor	Co_3W_3C	$W_2(C,O)$	22
HEP (ArHe)	21	25	4	Co_3W_3C = 4, others = 4	(d)	25-27
	29	26	42	Trace Co_3W_3C	...	24
VPS (ArHe & ArH_2)	Major	Trace	...	Traces	...	22
HVOF-DJ	35	27	34	Co_3W_3C = 4		25, 27
	44	35	17	Trace Co_3W_3C	...	24
HVOF Jet Kote	Major	Significant	...	Minor Co_3W_3C	Traces $Co_3W_9C_4$	7
	Major	Trace(e)	...	Significant	...	30
	Major	Trace	...	Traces	...	22
HVOF JP-5000(f)	Major	Trace	...	Minor	...	28

(a) The detailed analysis revealed relatively large amounts of tungsten in the semiamorphous cobalt binder phase. The numbers given represent the best of four coatings. (b) WC-Co powder size used was ~5-45 μm (type Metco 71 VF NS(g)). (c) This large percentage was attributed by Ramnath and Jayaraman (Ref 19) to both the lower relative starting %C in the fused and crushed powder as compared to the other types, as well as the fact that some η-phase is present in the powder already. (d) Nerz et al. (Ref 27) found that the coatings produced using cast and crushed powders exhibited considerably more evidence of amorphicity in the XRD-spectra, than did coatings produced with sintered and crushed, or agglomerated and densified, powders. The amorphous content of the high-energy plasma sprayed (cast crushed) coating was described as "very high," while that of the HVOF sprayed coating was described as "high." (e) A coating produced using a powder containing 5% C exhibited less W_2C than one produced from a powder containing 4% C, and some residual nonamorphous cobalt was even detected. (f) TAFA, Inc., Concord, NH. (g) Sulzer Metco, Westbury, NY.

Table 3(c) Published XRD results for WC-12 % Co coatings (sintered and crushed powders).
Numbers represent relative major peak intensities and NOT percentages, except in the cases of Ref 19 and 45, where percentages were calculated.

Process	WC	W_2C	W	$M_6C, M_{12}C$	Others	Reference
Powder	Major	...	...	Minor Co_6W_6C	Trace fcc cobalt	19, powder size 15-45 μm
	93	...	...	...	Co = 7 (fcc)	25-27
	Major	...	...	Minor Co_6W_6C	...	16, 22(b)
	Major	...	...	Trace Co_3W_3C	No cobalt(a)	14, 41
	Major	Trace	...	Minor Co_3W_3C	...	44, % cobalt not stated, assumed 12% Co
	Major	...	...	Minor Co_3W_3C	...	51
	Major	...	...	...	Trace graphite, cobalt	28
APS	66%	18%	7%	...	9% WC_{1-x}	19
(ArH_2)	Major	Minor	Trace	...	Traces $W_2(C,O)$	22
APS (ArHe)	Major	...	...	...	...	22
APS-9M (Ar)	Trace	Trace	Major	...	Traces free carbon	41
APS SG-100	Minor	Minor	Major	...	...	14(c)
APS at Mach 1.6	Minor	Minor	...	Major: Co_3W_3C	...	44
High-energy plasma	85-86	6	4	5	...	25-27
	80-85	7-10	...	7-10 Co_3W_3CV	...	32
VPS	Major	Trace	...	Minor/trace	...	22
	Major	Trace	Trace	...	...	23
HVOF-JP	Major	Trace	...	Minor Co_3W_3C	...	44
HVOF-DJ	78	12	7	3	...	27
	80-85	7-10	...	7-10 Co_3W_3C	...	32
HVOF-Jet Kote	Major	Trace	...	Trace Co_3W_3C	...	16
	Major	...	...	...	...	22
	Major	Trace	...	...	...	41

(a) Li et al. (Ref 41) state that the matrix phase is Co_3W_3C instead of cobalt. (b) Mazars et al. (Ref 22) used Amperit 515(d), size about 5-45 μm. (c) Powder (AI 1001) may be cast and crushed, it contained 4% C, but it is described as sintered and crushed. (d) H.C. Starck GmbH & Co., Singapore.

Table 3(d) Published XRD results for WC-12% Co (agglomerated powder types)
Numbers represent relative major peak intensities and NOT percentages.

Powder	Process	WC	W_2C	W	$M_6C, M_{12}C$	Others (trace)	Reference
Agglomerated only	Powder	Major	Minor(a)	...	...	hcp cobalt	19
	APS (ArH_2)	69%	24%	5%	...	2% WC_{1-x}	19
Agglomerated and sintered? (type Metco 74SF(b))	Powder	ND	ND	ND	ND	ND	45
	APS (ArH_2)	20%	34%	34%	...	2.3% Co	45
	APS (ArHe)	48%	9%	9%	...	3.9% Co	45
Not stated, possibly agglomerated and sintered	Powder	Major	Minor	...	...	...	34
	APS-F4	Major	Major	Minor	...	...	
	VPS-F4	Major	Minor	...	...	...	
	HVOF Jet Kote(c)	Major	Major	Minor	...	...	(d)
Agglomerated, sintered, and densified	Powder	Major	...	...	...	Cobalt (fcc)	19, 52
		89	...	...	...	Cobalt = 11 (fcc)	25-27
		Major	...	...	...	Cobalt (fcc)	53
		Major	Trace	...	Trace Co_6W_6C	Cobalt (fcc)	2
		Major	...	...	...	Cobalt (fcc)	16, 30
		Major	Trace	...	...	...	7, 23
		Major	Minor/trace	...	...	Cobalt (fcc)	12, 13
	APS (ArH_2)	72%	21%	6%	...	1% WC_{1-x}	19
	APS (ArHe)	Major	Minor	...	Traces	WC_{1-x}	2
	High-energy plasma	83	4	5	8	...	25, 27
	VPS-F4	Major	Trace	Trace	...	...	23
	VPS-F4	Major	Trace	...	...	...	50
	D-gun	Major	Trace	...	...	...	
	HVOF-DJ	80-81	5	9	6		25-27
	HVOF-Jet Kote	Major	Minor	...	Trace Co_3W_3C	...	7
		Major	Trace	...	...	...	16
		Major	Trace	...	Traces	Cobalt	30
	HVOF-CDS	Major	Significant	Minor	Trace Co_3W_3C, Co_3W_9C	...	47
		52	43	5	Present, not detected due to nanosize	...	53(e)
		54	23	23	...	...	
		Major	Minor	...	Trace Co_3W_3C	...	23
		Major	Minor	...	...	...	50
		Major	Minor/trace	Trace	...	...	12

(a) Orthorhombic W_2C. (b) Sulzer Metco, Westbury, NY. (c) These authors observed hcp cobalt in clad and agglomerated (spray dried) WC-12%Co powders, but not in cast and crushed, agglomerated and sintered, or dense sintered powders. (d) According to Wayne and Sampath (Ref 34), the larger-than-expected degree of decarburization in this HVOF coating can be attributed to oxidizing conditions in the flame. (e) Deloro Stellite, Goshen, IN.

Table 3(e) Summary of phase composition trends for 12% Co materials, taken from Tables 3(a-d)

Material	WC	W_2C	W	$M_6C, M_{12}C$	Others
Cast and crushed powders	Primary phase	Minor or significant	None or minor	Trace or minor	Usually none
Sintered and crushed powders	Primary phase	None or trace	None	None or minor	None or trace fcc cobalt
Agglomerated powders	Primary phase	None or trace	None	Usually none	Traces of cobalt
Plasma sprayed cast and crushed powder	Usually primary, but sometimes minor phase	Varies, minor or major phase	Minor, sometimes major phase	Trace or minor	Occasionally, traces of tungsten, $Co_3W_9C_4$ or $W_2(C,O)$
HVOF-deposited cast and crushed powder	Primary phase	Usually trace, but sometimes significant	Usually trace, but sometimes significant	Usually trace, sometimes significant	Occasionally, traces of $Co_3W_9C_4$
Plasma sprayed sintered and crushed powder	Usually primary phase, but in some cases minor phase with tungsten or Co_3W_3C as primary phase	Trace or minor phase	Usually none or traces, but sometimes the primary phase	Usually none or traces, (in one case, primary phase)	Usually none, occasionally trace
HVOF-deposited sintered and crushed powder	Primary phase	Trace or minor phase	Usually none	Trace or minor	None
All coatings from agglomerated powders	Usually primary phase	Varies from minor to significant	Varies from none to minor	None, or traces	None, or traces of cobalt

Table 4(a) Published XRD results for WC-17% Co coatings using sintered and crushed powders

Powder	Process	WC	W_2C	W	$M_6C, M_{12}C$	Others (trace)	Reference
Sintered and crushed	Powder	Major	...	...	Trace	Cobalt	33
		Major	...	...	Traces	...	22(a)
		Major	...	...	...	Cobalt	49
Not stated, possibly sintered and crushed	Powder	Major	...	...	...	Cobalt	48
	VPS	Major	...	...	...	Cobalt	
	APS	Minor	Major	...	...	WO_3, WC_{1-x}	
Sintered and crushed	APS (ArHe)	Major	...	...	...	...	22
	APS (ArH_2)	Major	Minor	Minor	...	$W_2(C,O)$	22
	VPS (ArHe)	Major	...	...	Traces	...	22
	VPS (ArH_2)	Major	Trace	...	Trace/minor	...	22
	HVOF-Jet Kote	Major	...	...	...	...	22
	APS	...	Trace	Major	...	CoO, WC_{1-x}	70
	APS	Major	Major	...	...	...	49
	LPPS	Minor	Major	...	...	CoO	49
	D-gun	Major	Major	Minor	...	...	70
	D-gun	Major	Significant	Significant	Significant	...	33
	HVOF-DJ	Major	...	...	...	...	70

(a) Mazars et al. (Ref 22) found that the finer (5-25 μm) version of this 5-45 μm powder, from the same manufacturer (Amperit 525(b)), contained only WC and cobalt. (b) H.C. Starck GmbH & Co., Singapore.

Table 4(b) Published XRD results for WC-17% Co coatings using agglomerated powders

Powder	Process	WC	W_2C	W	$M_6C, M_{12}C$	Others (trace)	Reference
Not stated, possibly agglomerated and sintered	Powder	Major	...	...	...		34
	APS-F4	Major	Major	Minor	...		
	VPS-F4	Major	Minor	Minor	...		
	HVOF-Jet Kote	Major	Major	Minor	...		(a)
Agglomerated, sintered, and densified	Powder	Major	...	...	...	...	7, 22, 71
		Major	Trace	...	Trace	Cobalt	33
		Major	...	...	Trace Co_6W_6C	Cobalt	40
		Major	...	...	Trace Co_3W_3C	...	23
		Major	...	...	...	Cobalt (hcp and fcc), Co_3W	2
		Major	...	...	...	fcc cobalt	13, 41
Agglomerated, sintered, and densified (AMDRY 983/1983 (c))	APS-F4	Major	Trace	Trace	Trace Co_3W_3C	...	23
	APS-F4	Major	Trace	...	Traces	...	40
	APS-F4	Major	Trace	...	Trace M_6C	...	50
	VPS-F4	Major	Trace	...	Trace Co_3W_3C	...	23
	VPS-F4	Major	Trace	...	Trace Co_3W_3C	Trace $Co_3W_9C_4$	40
	VPS-F4	Major	Trace	...	Trace Co_3W_3C	Trace cobalt	
Agglomerated, sintered, and densified (AMDRY 983(c) & JK7117)(d)	APS (ArHe)	Major	...	...	Trace	...	22
	APS (ArH_2)	Major	Minor	Minor	...	$W_2(C,O)$	
	VPS (ArHe)	Major	...	...	...	...	
	VPS (ArH_2)	Major	...	...	Trace	...	
	HVOF-Jet Kote	Major	...	...	...	...	
Agglomerated, sintered, and densified	APS-9M (ArHe)	Major	Trace	...	Minor	fcc cobalt, WC_{1-x}	2
Agglomerated and sintered	APS-9M (Ar)	Major	Trace	Minor	...	Free carbon	41
Agglomerated, sintered, and densified	HVOF-Jet Kote	Major	Minor	...	Trace Co_3W_3C	...	7, 22
		Major	...	...	...	...	41
		Major	Trace	Trace	...	Free carbon	40, 50
	HVOF-CDS	Major	Trace	...	Trace or no Co_3W_3C	...	13, 23
	D-gun	Major	...	...	Trace M_6C	...	50
		Major	...	...	Trace Co_3W_3C	...	23
		Major	Trace	None or trace	Trace	...	33(b)

(a) According to Wayne and Sampath (Ref 34), the larger-than-expected degree of decarburization in this HVOF coating can be attributed to oxidizing conditions in the flame. (b) These authors noted that finer powders showed a greater tendency to WC-transformation during spraying. (c) Sulzer Metco, Westbury, NY. (d) Deloro Stellite, Goshen, IN.

In HVOF spraying, it has likewise been shown that there is less retained WC in the coatings when a higher flame temperature (influenced by the flame stoichiometry) or greater standoff distance has been used (e.g., Ref 17). In general terms, therefore, decreasing the spray jet energy content and/or increasing its velocity (i.e., decreasing the time available for the reactions to occur) limits the extent of decarburization (e.g., Ref 24, 44, 63). Fincke et al. (Ref 44) point out that in the HVOF process, the temperatures are too low for the decarburization of WC into W_2C, CO, and CO_2 to occur to an appreciable extent, while the rate of the reactions between the binder and the WC are limited by diffusion. On the other hand, temperatures are very high in the plasma jet, and both the decarburization reactions and the binder-WC reactions can proceed very rapidly. This, coupled with the fact that HVOF gas jets entrain less air than APS plasma jets, as shown by Fincke et al. (Ref 44), probably explains why HVOF sprayed coatings tend to exhibit a lower degree of decarburization than plasma sprayed coatings, provided optimized spray parameters are used. See, for example, Nerz et al. (Ref 24) and Table 3. Hackett and Settles (Ref 72) showed for the JP-5000 process that a significant proportion of the surrounding atmosphere is entrained in the HVOF jet, but that this does not affect the particle velocity or temperature significantly, nor is it a major source of coating oxidation. The JP-5000 gas jet appears to be "self-sheathing" due to a low-density region in the center of the gas jet, which limits oxidation. The temperature of the coating surface appears to be the major factor affecting coating oxidation, because most of the oxidation occurs after particle solidification. This is confirmed by the work of Swank et al. (Ref 73, 74) who also provide detailed information regarding the gas and particle temperatures and velocities, as well as on the influence on these of the JP-5000 HVOF combustion parameters.

Increasing the oxygen-to-fuel ratio or the enthalpy of HVOF jets has been found to result in a greater loss of WC (e.g., Ref 41). The use of subsidiary cooling air jets has been found to increase decarburization of WC in both HVOF and plasma sprayed coatings (Ref 75), presumably due to the turbulence caused and hence the higher oxygen entrapment in the flame. Lenling et al. (Ref 60) describe a modified plasma spray gun whereby the alloy matrix feedstock is fed into the plasma jet upstream from WC-Co particles, thereby enabling sufficient melting of the matrix while significantly limiting the decarburization reaction of the WC phase.

The extent of WC loss in coatings is actually quite large when one considers the short reaction times available, of the order of 1 ms. While it is sometimes claimed that the velocity of the HVOF jet is one of the reasons for the lower extent of WC loss during HVOF spraying, it is interesting to note that the powder residence time in the gas jet is similar in both HVOF and air plasma spraying. In most HVOF spraying systems, WC-Co particles travel a distance of about 300 to 380 mm at about 315 m/s, and hence they spend ~1 ms in the gas jet before impacting on the surface. In the case of the JP-5000 HVOF process, the measured speed of 50 μm particles is higher than that reported for the earlier HVOF processes (500 m/s for a distance of 355 mm), and hence a dwell time of 0.7 ms is obtained (e.g., Ref 76). In APS, particles travel at 70 to 165 m/s for a distance of about 100 mm; that is, they spend ~0.6 to 1.4 ms in the plasma jet (data taken from Ref 38). Fincke et al. (Ref 44) in fact quote a higher dwell time (0.75 ms) for HVOF than for APS (0.3 ms). The primary advantage of the HVOF process is, therefore (Ref 44), the lower temperature, although of course the higher velocity can influence other properties such as adhesion and porosity.

In summary, therefore, attempts to limit the extent of WC decarburization during spraying usually involve one or more of the following:

- Reduction in the thermal energy available for melting the powder (by controlling the plasma parameters carefully or by using HVOF-type processes)
- Increase in the gas jet velocity (e.g., using the HVOF process)
- Prevention or limiting of the contact of the molten WC-Co particles with oxygen (spraying in reduced or inert atmospheres, spraying with an inert gas shroud, etc., e.g., Ref 31, 77). As Tables 3 and 4 show, however, this method does not have major advantages, and it is also expensive and impractical for most coating shops serving the industrial market.
- Addition of free carbon to the powder (Ref 31, and various patents)
- Covering the powder particle with a metal layer (Ref 78)

Based on the above, the HVOF process is expected to have significant advantages over plasma spraying for the deposition of sensitive materials such as WC, and it is well known that the HVOF process does in fact produce better coatings in most instances (e.g., Ref 44, 70).

Detailed experimental results are discussed in the paragraphs below.

General. Tables 3 and 4 summarize some of the published results of XRD measurements on various WC-Co powders and coatings and are discussed below. Direct comparison of the results is not realistic, because even when different researchers use the same spray system and powder, they are likely to use different spray parameters. The qualitative nature of XRD measurements should also be taken into account. Hence, Tables 3 and 4 serve only to indicate trends.

It may be noticed from the Tables that cobalt is not often detected by XRD. While most researchers do not cover this topic, several (Ref 13, 16, 19, 25, 27, 47, 49, 60, 63) have attributed it to the fact that the cobalt binder is mostly either amorphous or in the form of nanocrystalline $Co_xW_yC_z$ compounds, and hence the appearance of its intensity peaks is inhibited and is replaced by an amorphous "hump" in the XRD spectrum.

Powder Phase Composition (12%Co). The characteristics of the powder types containing 12% Co are:

- *Cast and crushed powders:* These feedstocks usually contain primarily WC, with significant amounts of W_2C, and minor or trace amounts of tungsten and Co_3W_3C (the latter is softer than WC, Ref 77). Rangaswamy and Herman (Ref 2) stated for a well-known brand of cast and crushed powder (71NS) that "the metallic binder contains dissolved tungsten throughout" due to a "high-temperature sintering step during powder production." One investigation also detected $Co_3W_9C_4$ in a cast and crushed powder. De Villiers Lovelock, Kinds, and Young (Ref 18) found that for three cast and crushed powders, all of them except AI 1101 contained significant amounts of W_2C, all of them contained trace amounts of Co_3W_3C, none contained tungsten, and one (WC-432) contained traces of $Co_3W_9C_4$. From the

work of Kreye et al. (Ref 30), it might be concluded that the investigations where no W_2C was detected may have been conducted on cast and crushed powders with higher carbon contents (typically 5% versus 4%), but all the workers listed in Table 2(a) used 4% C powders, and some of these appear in Table 3(a) with no W_2C detected.

- *Sintered and crushed powders:* These feedstocks contain primarily WC with no W_2C or tungsten, and minor or trace amounts of cobalt and Co_6W_6C/Co_3W_3C. According to Wagner et al. (Ref 42), the ternary phases form on the WC/Co boundaries during the sintering step in the powder production process. One investigation listed in Table 3(c) detected fcc cobalt. De Villiers Lovelock, Kinds, and Young (Ref 18) investigated seven powders and found that all of them contained only WC and trace amounts of fcc cobalt, with in one case a trace of Co_3W_3C.
- *Agglomerated and densified powders:* These feedstocks contain primarily WC, with minor or trace amounts of Co_6W_6C/W_2C, but never tungsten. Presumably these phases originate during sintering or densification. A number of workers detected fcc cobalt in these powders. De Villiers Lovelock, Kinds, and Young (Ref 18) found that for four powders from different suppliers, two contained WC plus trace fcc cobalt (WC-616 and Amperit 518), and two contained WC plus traces of W_2C and CoC_x.

Hence from the point of view of minimizing the non-WC phases in the starting powder, cast and crushed powders are undesirable. This is confirmed by the results shown in Tables 2(a) and 3 for the corresponding coatings (see also Ref 7, 23, 50). Cast and crushed powders are often used only when user specifications dictate it.

Powder Phase Composition (17% Co). The characteristics of the powder types containing 17% Co are:

- *Sintered and crushed powders:* These feedstocks contain primarily WC with no W_2C or tungsten, and minor or trace amounts of cobalt and Co_6W_6C/Co_3W_3C.
- *Agglomerated and densified powders:* These contain primarily WC, with minor or trace amounts of Co, Co_3W_3C, Co_6W_6C, and in one case W_2C, but never tungsten. One worker detected hcp cobalt in addition to fcc cobalt. This was also found by de Villiers Lovelock, Kinds, and Young (Ref 18) for one powder out of nine investigated, while traces of CoC_x were observed in two other powders. All of the others investigated by these authors contained only WC and traces of fcc cobalt.

Coating Phase Compositions—General Observations. From Tables 3 and 4, it is apparent that air plasma spraying always increases the proportion of non-WC carbide phases and amorphous content in the materials. HVOF and LPPS spraying have the same effect, but often to a lesser degree (see also Giordano et al., Ref 71; Slavin and Nerz, Ref 32; and Mutasim et al., Ref 77). For fused and crushed powders, the non-WC phases in the coatings are usually of similar type to those in the starting powder, except that their content has increased. This is particularly clear when comparing powder and coating results from the same workers. For sintered and crushed powders (Tables 3c and 4a), spraying often introduces W_2C and tungsten into the coating, and only seldom are the ternary phases that were present in the powders retained in the coatings. WC_{1-x}, CoO, WO_3, and $W_2(C,O)$ formed in the coatings in isolated cases. For agglomerated type powders (Tables 3d and 4b), spraying generally increases the W_2C content compared to the starting powder and sometimes introduces tungsten and/or traces of ternary Co-W-C phases into the coatings. Generally, however, WC remains the major crystalline phase.

Comparing the results from the same references in Tables 3 and 4 gives an indication of the effect of thermal spray process and choice of plasma gas type. On the other hand, the often large variation in the results published by different workers underlines the importance of controlling the processing conditions for any given process.

Most authors do not discuss the extent of amorphous phase formation during spraying, and there is insufficient published data to compare powder types in this regard. Significantly large amounts of amorphous phases are present in plasma sprayed coatings (Ref 22, 63, 71, 79), while HVOF coatings can be produced with almost no amorphous phase (Ref 20, 71) but can also display a significant amount of it (Ref 41, 42, 47, 53, 63, 79). D-gun coatings can also contain a significant amount of amorphous material (Ref 70).

Loss of Carbon During Spraying. Some of the observations published on less commonly used powder types are interesting. Li et al. (Ref 41) included a spherically shaped cast, crushed and fused powder in their work. The powder contained WC, W_2C, Co_3W_3C, and Co_6W_6C. The coatings, sprayed by Jet Kote HVOF and APS, contained WC, W_2C, Co_2W_4C, and tungsten, but no Co_3W_3C or Co_6W_6C. In the ternary phase diagram of Fig. 2, this implies the formation of η_2 at the expense of η and η_1, that is, an overall loss of carbon and cobalt. Strangely, free carbon was also detected in the coatings by XRD. In the HVOF coating this could be a residue from the acetylene and propylene fuel gas used, but in the plasma sprayed coating it is inexplicable.

The XRD results of Detering et al. (Ref 51) using sintered and crushed powder (result not included in Table 4) are also of interest. The plasma sprayed coatings contained WC, W_2C, and tungsten, while the powder contained only WC and Co_3W_3C. Once again, a shift during spraying to the tungsten-rich corner of the phase diagram is evident.

Chemical analysis confirms the results of XRD techniques, in that it almost always indicates a lower carbon content in thermally sprayed coatings than in the starting powders. Proportional loss of carbon can be as high as 38% in HVOF coatings (Ref 24), as high as 45% in well-sprayed APS coatings (Ref 5, 14, 27, 80) and as high as 50 to 66% in poorly sprayed coatings that contain dissolved WC phases (Ref 20, 24, 81). Similar results have been obtained for APS and HVOF sprayed WC-Ni coatings (Ref 46, 68), demonstrating that the effect is probably not binder-dependent, and similar loss of carbon has been reported in chrome carbide-base thermally sprayed coatings (e.g., Basinska-Pampuch and Gibas, Ref 56).

Mei et al. (Ref 82), who investigated the HVOF spraying of two nonstandard powders, found that a powder consisting of WC particles clad in cobalt exhibited more loss of WC than a sintered and crushed powder, showing that the cobalt cladding does not protect the WC from oxidation. Similar results were noted by Rangaswamy and Herman (Ref 2) for a plasma sprayed clad WC-Co. Possibly, in the case of clad powders, the cobalt melts and is "pulled off" the WC particle in flight (Ref 30, 42),

as is also evidenced by much lower deposition efficiencies for these powders due to a lack of adhesion on impact (Ref 83). Another possible explanation for the phenomenon, proposed by Basinska-Pampuch and Gibas (Ref 56), is that the WC dissolves in the molten cobalt layer during flight, and the small carbon atoms diffuse outward rapidly and are oxidized to CO/CO_2.

Basinska-Pampuch and Gibas (Ref 56), who used nonstandard blended and clad WC and Cr_3C_2-base powders, did not observe any reduction in decarburization due to the addition of binder metals/alloys. The effect of WC grain size outweighed all other factors, with a larger grain size resulting in less decarburization even when pure WC powder without any binder was sprayed. Li et al. (Ref 41, 65), who sprayed clad WC-18%Co powders with Jet Kote HVOF and APS, noted that the WC size in the powder was larger (about 18 μm) than in the other more commonly used powders. The powder contained only WC and α-cobalt. The XRD spectrum for the HVOF coating showed WC, carbon, and an unusually large amorphous hump, compared to other published data. The amorphous material recrystallized upon heat treatment in air at 873 K to Co_6W_6C, tungsten, cobalt, and free carbon (heat treatment at 673 K for 3 h had no effect). After treatment in vacuum at 1173 K for 0.5 h the coating contained only Co_6W_6C, cobalt, and free carbon, and the authors conclude, based on their further investigations, that the tungsten is used up to form Co_6W_6C, at a reaction temperature of about 1104 K. Apparently, the WC and the outer cobalt layer reacted during spraying to form an amorphous W-Co-C binder. Very few larger WC particles were observed in this HVOF coating, possibly due to the rebounding of larger WC particles upon impact (Ref 41, 65). The plasma sprayed coating from this clad powder exhibited WC, traces of W_2C, and some amorphous material, and was very porous; that is, there was less decarburization but also (inevitably) less melting/flattening of the powder particles.

Minimizing the Loss of Carbon During Spraying. Because the effect of non-WC phases on the wear and other properties is generally perceived to be negative (e.g., Ref 44), several researchers have investigated the possibility of inhibiting the extent of brittle W_2C and $Co_xW_yC_z$-phase formation, and some of the methods used have been described in section 4.1. In addition to these, alternative carbide compositions have also been proposed. It is well documented (see, for example, Ref 3) that TiC and TaC, with their cubic structures, can tolerate a much larger degree of decarburization than the hexagonal α-WC before they transform into other carbide phases. Schultrich et al. (Ref 52) investigated a series of plasma sprayed coatings produced using powders with a graduated W-to-(Ti,Ta) ratio in the carbide phase. Various binder alloys were used. They found that while WC decomposed almost completely to W_2C and tungsten (and in some cases even WC_{1-x}), the (W,Ti)C and (W,Ti,Ta)C phases remained cubic and became enriched with oxygen and nitrogen interstitial atoms that replaced the carbon atoms in the cubic lattice. Berger et al. (Ref 57) subsequently investigated the pin-on-disk wear properties of these coatings and found no improvement in the (W,Ti)C-Co coatings compared to the WC-Co coatings. This may be because TiC and TaC are quite brittle, compared to WC. They then investigated the effect of adding 0.5 to 1.2% additional carbon in the form of a graphite coating on the powder particles. Decarburization was significantly reduced, but, due to the presence of residual free carbon in the coating, wear rates were increased. They proposed that future work should focus on obtaining a balance between the prevention of decarburization and the presence of free carbon in the coatings.

5. Conclusions

Published findings regarding the microstructure and phase composition of WC-Co thermally sprayed coatings, produced from cast/crushed, sintered/crushed, and agglomerated/densified powders, have been summarized and compared. The loss of WC during thermal spraying and the resultant coating phase structure has been discussed in detail.

As far as the microstructure is concerned, porosity and WC size, distribution, and content are the most important factors. Published porosity values for the coatings vary between <0.2% and almost 20%. It is possible that metallographic preparation methods play a role in this large variation, but nevertheless the reported range illustrates the extremes that are obtainable. Porosity is generally higher for plasma sprayed coatings than for HVOF and D-gun coatings, as would be expected. It is consistently low (<2%) for HVOF coatings. For plasma sprayed coatings, it seems to decrease as the degree of melting (and hence the degree of WC loss during spraying) increases, indicating that the optimal coating structure for plasma sprayed coatings may involve a compromise between low porosity and more retained WC particles. This is also true to a lesser extent in D-gun and HVOF coatings (Ref 30, 33).

The WC grain size in cast/crushed WC-12%Co powders and the coatings produced from them is larger than that produced from other powder types. Cast/crushed powders exhibit greater loss of visible WC during spraying than the other powder types, and the sintered/crushed powder types appear to be the least susceptible to visible WC loss during spraying. This is confirmed by chemical analysis to measure total carbon loss during spraying. From the work of Mazars et al. (Ref 22) and others, it is clear that for all powders, the use of plasma gas compositions with higher thermal energy, such as ArH_2 plasmas instead of ArHe plasmas, leads to observably more loss and/or dissolution of visible WC in the microstructure.

Many researchers attribute variations in the properties (including wear resistance) of thermally sprayed WC-Co to the phase changes that occur in the material during spraying (see section 4.1). During plasma spraying, the WC-Co powder tends to undergo decarburization, oxidation, reduction by reaction with the H_2 in the plasma gas, and dissolution/reaction between the WC and the cobalt binder metal during spraying, resulting in the formation of hard and brittle phases such as W_2C, Co_3W_3C, Co_6W_6C, Co_2W_4C, $Co_3W_9C_4$, and even WO_3 and tungsten. The binder in thermally sprayed WC-Co coatings is often predominantly amorphous $Co/C/W/Co_xW_yC_z$ due to rapid postspraying solidification. Evidence of partial recrystallization of the amorphous binder phase by means of nucleation of crystallites at the WC/Co interface has been documented (Ref 11, 47). These phases can also crystallize from the melt during solidification (Ref 56, 58), sometimes in the form of very fine (nano) crystallites (Ref 11). The amorphous Co-W-C binder alloy has also

been observed to recrystallize during heat treatment of coatings above about 900 K.

The changes occurring in WC-Co during spraying are collectively referred to as "decarburization," because they are generally accompanied by a decrease of up to 50% in the total carbon content. The free carbon thus liberated can be eliminated from the coating entirely by oxidation to CO or CO_2 or can remain dissolved in the cobalt matrix after solidification. Metallic tungsten W or W_2C can also be dissolved in the cobalt binder or be present on the surface of WC particles. Similar effects occur during HVOF spraying, but usually to a much lesser degree due to the lower temperatures involved (Ref 44).

The extent of the WC transformation during spraying depends on the starting powder type (size, morphology, carbide size), the type of spray process, the amount of oxygen in the environment, and the spray parameters (Ref 34, 41, 44). For example, in plasma spraying, the higher the enthalpy of the plasma gas, the more WC decarburization and reaction with the binder phase can be expected, because more thermal energy is available to drive the process. In HVOF spraying, it has likewise been shown that there is less retained WC in the coatings when a higher flame temperature (influenced by the flame stoichiometry) or greater standoff distance has been used (e.g., Ref 17). In general terms, therefore, decreasing the spray jet energy content and/or increasing its velocity (i.e., decreasing the time available for the reactions to occur) limits the extent of decarburization. Increasing the oxygen-to-fuel ratio or the enthalpy of HVOF jets has been found to result in a greater loss of WC (e.g., Ref 41). The use of subsidiary cooling air jets has been found to increase decarburization of WC in both HVOF and plasma sprayed coatings (Ref 75), presumably due to the turbulence caused, and the higher oxygen entrapment in the flame.

Whether the formation of non-WC carbide phases is beneficial or detrimental for wear resistance appears to depend on the details of the tribosystem under consideration, and possibly also on the detailed coating composition and microstructure, because there are conflicting reports in the literature. Generally however it is considered detrimental. Some HVOF coatings have even been observed to perform better than sintered hard metals of comparable composition in mild hydroabrasive wear as well as three-body abrasion (dry sand rubber wheel) tests. Other workers have found the coatings to wear at a higher rate than their sintered counterparts (e.g., Ref 61). This aspect is, however, beyond the scope of the current article and will be dealt with in a subsequent review.

Acknowledgment

The author is indebted to Prof. Silvana Luyckx for her detailed feedback after reading the first and second drafts of the manuscript and to Prof. Frank Nabarro for his encouragement of the work.

References

1. H.E. Exner, Physical and Chemical Nature of Cemented Carbides, *Int. Met. Rev.*, Vol 24, 1979, p 149
2. S. Rangaswamy and H. Herman, Metallurgical Characterization of WC-Co Coatings, *Advances in Thermal Spraying*, Pergamon Press, 1986, p 101-110
3. W. Schedler, *Hard Metals for Practical Users* (original title: *Hartmetall für den Praktiker*), VDI-Verlag, Düsseldorf, 1988, p 5-29 (in German)
4. H. Baker and H. Okamoto, *Alloy Phase Diagrams*, Vol 3, *ASM Handbook*, ASM International, 1992, p 2.115
5. D. Tu, S. Chang, C. Chao, and C. Lin, Tungsten Carbide Phase Transformation During the Plasma Spray Process, *J. Vac. Sci. Technol.*, Vol A3 (No. 6), 1985, p 2479-2482
6. P. Rautala and T. Norton, *Proc. 1st Plansee Seminar*, Plansee, Reutte, Austria, 1952, p 303-316
7. G. Barbezat, E. Müller, and B. Walser, Metallurgy and Properties of Tungsten Carbide-Cobalt Coatings Produced using the Jet Kote Process, *VDI-Ber.*, Vol 670, 1988, p 853-872 (in German)
8. C.B. Pollock and H.H. Stadelmaier, The Eta Carbides in the Fe-W-C and Co-W-C Systems, *Metall. Trans.*, Vol 1, 1970, p 767-770
9. V.K. Sarin, Morphology of Eta Phase in Cemented WC-Co Alloys, *Modern Developments Powder Metallurgy*, Vol 10, Metal Powder Industries Federation, 1977, p 553-565
10. L. Åkesson, An Experimental and Thermodynamic Study of the Co-W-C System in the Temperature Range 1470-1700 K, *Science of Hard Materials*, Proc. Int. Conf., 23-28 Aug (Jackson, WY), Plenum Press, 1983, p 71-82
11. C. Verdon, "Microstructure and Erosion Resistance of WC-M Coatings Deposited by HVOF Thermal Spraying" (original title: "Microstructure et Résistance à l'Érosion de Revêtements WC-M Déposés par Projection Thermique HVOF"), Ph.D. Thesis No. 1393, École Polytechnique Fédérale de Lausanne (EPFL), Switzerland, 1995 (in French)
12. J.M. Guilemay, J. Nutting, and J.M. de Paco, Characterization of Three WC + 12Co Powders and the Coatings Obtained by High-Velocity-Oxygen-Fuel Spraying, *Proc. Fourth European Conf. Adv. Mater. Processe (EUROMAT)*, 25-28 Sept 1995 (Venice), Assoc. Italiana di Metallurgica, Milan, 1996, p 395-398
13. J.M. Guilemay and J.M. de Paco, Structure/Properties Relationship of WC + Co Coatings Obtained by HVOF Spraying Using Starting Powders with Different Content in the Metallic Matrix, No. DVS 175, *Proc. Therm. Spray Conf. TS '96*, Deutsche Verband für Schweisstechnik, Düsseldorf, 1996, p 390-393
14. D.J. Varacalle, G.R. Smolik, G.C. Wilson, G. Irons, and A. Walter, An Evaluation of Tungsten Carbide-Cobalt Coatings Fabricated with the Plasma Spray Process, *Protective Coatings: Processing and Characterization*, R.M. Yazici, Ed., The Minerals, Metals and Materials Society, 1990, p 121-134
15. G. Barbezat, High-Velocity Flame Spraying of Protective Coatings, *Metalloberfläche*, Vol 43 (No. 10), 1989, p 459-466 (in German)
16. T. Tomita, Y. Takatani, Y. Kobayashi, Y. Harada, and H. Nakahira, Durability of WC/Co Sprayed Coatings in Molten Pure Zinc, *ISIJ Int.*, Vol 33 (No. 9), 1993, p 982-988; first published in *Tetsu-to-Hagané*, Vol 78, 1992 (in Japanese)
17. K. Korpiola and P. Vuoristo, Effect of HVOF Gas Velocity and Fuel to Oxygen Ratio on the Wear Properties of Tungsten Carbide Coating, *Thermal Spray: Practical Solutions for Engineering Problems*, C.C. Berndt, Ed., ASM International, 1996, p 177-184
18. H.L. de Villiers Lovelock, J. Kinds, and P.M. Young, Characterization of WC 12%Co Thermal Spray Powders and HP/HVOF Coatings, *Powder Metall.*, accepted for publication
19. V. Ramnath and N. Jayaraman, Characterization Wear Performance of Plasma Sprayed WC-Co Coatings, *Mater. Sci. Technol.*, Vol 5, 1989, p 382-388
20. H.J. Kim, Y.G. Kweon, and R.W. Chang, Wear and Erosion Behavior of Plasma-Sprayed WC-Co Coatings, *J. Therm. Spray Technol.*, Vol 3 (No. 2), 1994, p 169-178
21. D.J. Varacalle, Jr., E. Acosta, J. Figert, M. Syma, J. Worthington, and D. Carrillo, Experimental/Analytical Investigations of Air Plasma Spray Tungsten Carbide-Cobalt Coatings at Kelly Air Force Base, *Thermal*

Spray: Practical Solutions for Engineering Problems, C.C. Berndt, Ed., ASM International, 1996, p 699-707

22. P. Mazars, D. Manesse, and C. Lopvet, Structure of Tungsten Carbide Coatings Obtained by Different Spray Processes, *Advances in Thermal Spraying,* Pergamon Press, 1986, p 111-120; also published in *Soudage Tech. Connexes,* Vol 41 (No. 1-2), 1987, p 36-42 (in French)
23. T.A. Mäntylä, K.J. Niemi, P.M.J. Vuoristo, G. Barbezat, and A.R. Nicoll, Abrasion Wear Resistance of Tungsten Carbide Coatings Prepared by Various Thermal Spraying Techniques, *Second Plasma-Technik Symposium,* Vol 1, S. Blum-Sandmeier, H. Eschnauer, P. Huber, and A. Nicoll, Ed., Sulzer Metco AG, Wohlen, Switzerland, 1991, p 287-297
24. J.E. Nerz, B.A. Kushner, and A.J. Rotolico, Effects of Deposition Methods on the Physical Properties of Tungsten Carbide-12 wt% Cobalt Thermal Spray Coatings, *Protective Coatings: Processing and Characterization,* R.M Yazici, Ed., The Minerals, Metals and Materials Society, 1990, p 133-143
25. J.E. Nerz, B.A. Kushner, and A.J. Rotolico, Relationship between Powder Processing and Deposition Methods for Aircraft Grade Tungsten Carbide-Cobalt Coatings, Publication No. DVS 130, *Proc. Therm. Spray Conf. TS90,* 29-31 Aug 1990 (Essen, Germany), Deutsche Verband für Schweisstechnik, 1992, p 47-51; also published in *Proc. Asian Aerospace Conf.,* 1990, Singapore
26. M.R. Dorfman, B.A. Kushner, J. Nerz, and A.J. Rotolico, A Technical Assessment of High Velocity Oxygen-Fuel versus High Energy Plasma Tungsten Carbide-Cobalt Coatings for Wear Resistance, *Proc. 12th Int. Thermal Spray Conf.* (London), I.A. Bucklow, Ed., The Welding Institute, London, 1989, p 108.1-108.12
27. J.E. Nerz, B.A. Kushner, and A.J. Rotolico, Characterization of Tungsten Carbide Coatings as a Function of Powder Manufacturing and Deposition Technologies, *High Performance Ceramic Films and Coatings,* Vol 67, *Materials Science Monograph,* 1991, p 27-36
28. S.Y. Hwang, B.G. Seong, and M.C. Kim, Characterization of WC-Co Coatings Using HP/HVOF Process, *Thermal Spray: Practical Solutions for Engineering Problems,* C.C. Berndt, Ed., ASM International, 1996, p 107-112
29. H. Kreye, Optimization and Control of the Spray Conditions in the Jet Kote Process, *Thermal Spray Technology—New Ideas and Processes,* D.L. Houck, Ed., ASM International, 1989, p 39-45
30. H. Kreye, D. Fandrich, H.H. Müller, and G. Reiners, Microstructure and Bond Strength of WC-Co Coatings Deposited by Hypersonic Flame Spraying (Jet Kote Process), *Advances in Thermal Spraying,* Proc. 11th Int. Thermal Spray Conf., 8-12 Sept 1986 (Montreal, Canada), Pergamon Press, 1986 p 121-128
31. Y. Arata, A. Ohmori, and E. Gofuku, WC-Co High Energy Thermal Sprayed Coatings, *Trans. Jpn. Weld. Res. Inst.,* Vol 14 (No. 2), 1985, p 67-73
32. T.P. Slavin and J. Nerz, Material Characteristics and Performance of WC-Co Wear Resistant Coatings, *Thermal Spray Research and Applications,* T.F. Bernecki, Ed., ASM International, 1991, p 159-165
33. P. Vuoristo, K. Niemi, A. Mäkelä, and T. Mäntylä, Spray Parameter Effects on Structure and Wear Properties of Detonation Gun Sprayed WC + 17%Co Coatings, *Thermal Spray: Research, Design, and Applications,* C.C. Berndt and T.F. Bernecki, Ed., ASM International, 1993, p 173-178
34. S.F. Wayne and S. Sampath, Structure/Property Relationships in Sintered and Thermally Sprayed WC-Co, *J. Therm. Spray Technol.,* Vol 1 (No. 4), 1992, p 307-315
35. K. Niemi, P. Vuoristo, T. Mäntylä, G. Barbezat, and A.R. Nicoll, Abrasion Wear Resistance of Carbide Coatings Deposited by Plasma and High Velocity Combustion Processes, *Thermal Spray: International Advances in Coatings Technology,* C.C. Berndt, Ed., ASM International, 1992, p 685-689
36. A. Karimi, Ch. Verdon, J.L. Martin, and R.K. Schmid, Slurry Erosion Behaviour of Thermally Sprayed WC-M Coatings, *Wear,* Vol 186-187, 1995, p 480-486
37. W.J. Jarosinski, M.F. Gruninger, and C.H. Londry, Characterization of Tungsten Carbide Cobalt Powders and HVOF Coatings, *Thermal Spray: Research, Design, and Applications,* C.C. Berndt and T.F. Bernecki, Ed., ASM International, 1993, p 153-157
38. N. Wagner, K. Gnädig, H. Kreye, and H. Kronewetter, Particle Velocity in Hypersonic Flame Spraying of WC-Co, *Surf. Technol.,* Vol 22, 1984, p 61-71
39. D.C. Crawmer, J.D. Krebsbach, and W.L. Riggs, Coating Development for HVOF Process Using Design of Experiments, *Thermal Spray: International Advances in Coatings Technology,* C.C. Berndt, Ed., ASM International, 1992, p 127-136
40. Y. Naerheim, C. Coddet, and P. Droit, Effect of Thermal Spray Process Selection on Tribological Performance of WC-Co and Al_2O_3-TiO_2 Coatings, *Surf. Eng.,* Vol 11 (No. 1), 1995, p 66-70
41. C.-J. Li, A. Ohmori, and Y. Harada, Effect of Powder Structure on the Structure Of Thermally Sprayed WC-Co Coatings, *J. Mater. Sci.,* Vol 31, 1996, p 785-794
42. N. Wagner, H. Kreye, and H. Kestel, Production of Wear Resistant WC-Co Coatings Using Hypersonic Flame Spraying, *Z. Werkstoffech.,* Vol 16, 1985, p 55-60 (in German)
43. M.S.A. Khan and T.W. Clyne, Microstructure and Abrasion Resistance of Plasma Sprayed Cermet Coatings, *Thermal Spray: Practical Solutions for Engineering Problems,* C.C. Berndt, Ed., ASM International, 1996, p 113-122
44. J.R. Fincke, W.D. Swank, and D.C. Haggard, Comparison of the Characteristics of HVOF and Plasma Thermal Spray, *Thermal Spray Industrial Applications,* C.C. Berndt and S. Sampath, Ed., ASM International, 1994, p 325-330
45. J. Subrahmanyam, M.P. Srivastava, and R. Sivakumar, Characterization of Plasma Sprayed WC-Co Coatings, *Mater. Sci. Eng.,* Vol 84, 1986, p 209-214
46. M. Witold, Plasma Gun Spraying of WC and WC-Co Powders, *Powloki Ochr.,* Vol 2 (No. 2), 1974, p 13-23
47. A. Karimi, Ch. Verdon, and G. Barbezat, Microstructure and Hydroabrasive Wear Behaviour of High Velocity Oxy-Fuel Thermally Sprayed WC-Co(Cr) Coatings, *Surf. Coat. Technol.,* Vol 57, 1993, p 81-89
48. H. Takigawa, M. Hirata, M. Koga, M. Itoh, and K. Takeda, Applications of Hard Coating by Low-Pressure Plasma Spray, *Surf. Coat. Technol.,* Vol 39/40, 1989, p 127-134
49. D. Ghosh, D. Lamy, T. Sopkow, and I. Smuga-Otto, The Effects of Plasma Spray Parameters and Atmospheres on the Properties and Microstructure of WC-Co Coatings, *Proc. 24th Int. SAMPE Technical Conf.,* 20-22 Oct 1992 (Toronto), Vol 24, T.S. Reinhardt, Ed., Society for Advancement of Material and Process Engineering, 1992, p T28-T42
50. G. Barbezat, A.R. Nicoll, and A. Sickinger, Abrasion, Erosion and Scuffing Resistance of Carbide and Oxide Ceramic Thermal Spray Coatings for Different Applications, *Wear,* Vol 162-164, 1993, p 529-537
51. B.A. Detering, J.R. Knibloe, and T.L. Eddy, Occurrence of Tungsten Plasma in Plasma Spraying of WC/Co, *Thermal Spray Research and Applications,* T.F. Bernecki, Ed., ASM International, 1991, p 27-31
52. B. Schultrich, L.-M. Berger, J. Henke, and A. Oswald, Influence of Carbide Powder Composition on Decarburization During Air Plasma Spraying, *Second Plasma-Technik Symposium,* Vol 2, S. Blum-Sandmeier, H. Eschnauer, P. Huber, and A. Nicoll, Ed., Sulzer Metco AG, Wohlen, Switzerland, 1991, p 363-371
53. A. Karimi and Ch. Verdon, Hydroabrasive Wear Behaviour of High Velocity Oxyfuel Thermally Sprayed WC-M Coatings, *Surf. Coat. Technol.,* Vol 62, 1993, p 493-498
54. M.E. Vinayo, F. Kassabji, J. Guyonnet, and P. Fauchais, Plasma Sprayed WC-Co Coatings: Influence of Spray Conditions (Atmospheric and Low

Pressure Plasma Spraying) on the Crystal Structure, Porosity and Hardness, *J. Vac. Sci. Technol.*, Vol A3 (No. 6), 1985, p 2483-2489

55. A. Tronche and P. Fauchais, Hard Coatings (Cr_2O_3, WC-Co) Properties on Aluminium or Steel Substrates, *Mater. Sci. Eng.*, Vol 92, 1987, p 133-144
56. S. Basinski-Pampuch and T. Gibas, Observations on Some Plasma-Sprayed Metal Carbides, *Ceram. Int.*, Vol 3 (No. 4), 1977, p 152-158
57. L.-M. Berger, B. Schultrich, A. Oswald, and H. Preiss, Influence of Carbide Powder Composition on Decarburization and Properties of Air Plasma Sprayed Coatings, *Thermal Spray: International Advances in Coatings Technology*, C.C. Berndt, Ed., ASM International, 1992, p 253-258
58. M.G.S. Naylor, *Development of Wear-Resistant Ceramic Coatings for Diesel Engine Components*, Vol 1, Report DE 92 041382, Oak Ridge National Laboratory Reference ORNL/Sub/87-SA581/1, National Technical Information Service, U.S. Dept. of Commerce, 1992
59. Ch. Heinzelmaier and K.K. Schweitzer, WC-Co Coatings for Protection against Hammer Wear in Flight Engines, Publication No. DVS 130, *Proc. Thermal Spray Conf. TS90*, 29-31 Aug 1990 (Essen, Germany), Deutsche Verband für Schweisstechnik, Düsseldorf, 1990, p 51-54
60. W.J. Lenling, M.F. Smith, and J.A. Henfling, Process for Producing Plasma Sprayed Carbide-Based Coatings with Minimal Decarburization and Near Theoretical Density, *Thermal Spray Research and Applications*, T.F. Bernecki, Ed., ASM International, 1991, p 451-455
61. P.L. Kuhanen and P.O. Kettunen, Comparison of Plasma and Detonation Gun Sprayed Tungsten Carbide-Cobalt Coatings, Publication No. DVS 152, *Proc. Thermal Spray Conf. TS93*, 3-5 March 1993, (Aachen, Germany), Deutsche Verband für Schweisstechnik, Düsseldorf, 1993, p 100-102
62. V.V. Sobolev, J.M. Guilemay, and J.A. Calero, Formation of Structure of WC-Co Coatings on Aluminium Alloy Substrate During High-Velocity Oxy-Fuel (HVOF) Spraying, *J. Therm. Spray Technol.*, Vol 4 (No. 4), 1995, p 401-407
63. J.E. Nerz, B.A. Kushner, and A.J. Rotolico, Microstructural Evaluation of Tungsten Carbide-Cobalt Coatings, *J. Therm. Spray Technol.*, Vol 1 (No. 2), 1992, p 147-152
64. L.-M. Berger, P. Vuoristo, T. Mäntylä, W. Kunert, W. Lengauer, and P. Ettmayer, Microstructure and Properties of WC-Co-Cr Coatings, *Thermal Spray: Practical Solutions for Engineering Problems*, C.C. Berndt, Ed., ASM International, 1996, p 97-106
65. C.-J. Li, A. Ohmori, and Y. Harada, Formation of an Amorphous Phase in Thermally Sprayed WC-Co, *J. Therm. Spray Technol.*, Vol 5 (No. 1), 1996, p 69-73
66. J.M. Guilemay, V.V. Sobolev, J. Nutting, Z. Dong, and J.A. Calero, Thermal Interaction between WC-Co Coating and Steel Substrate in Process of HVOF Spraying, *Scr. Metall. Mater.*, Vol 31 (No. 7), 1994, p 915-920
67. J. Nutting, J.M. Guilemay, and Z. Dong, Substrate/Coating Interface Structure of WC-Co HVOF Sprayed Coatings on to Low Alloy Steel, *Mater. Sci. Technol.*, Vol 11 (No. 9), 1995, p 961-966
68. J.M. Guilemay, J. Nutting, J.R. Miguel, and Z. Zong, Microstructure Characterization of WC-Ni Coatings Obtained by HVOF Thermal Spraying, *Scr. Metall. Mater.*, Vol 33 (No. 1), 1995, p 55-61
69. L.E. McCandlish, B.H. Kear, B.K. Kim, and L.W. Wu, Low Pressure Plasma Sprayed Coatings of Nanophase WC-Co, *Protective Coatings: Processing and Characterization*, R.M. Yazici, Ed., The Minerals, Metals and Materials Society, 1990, p 113-119
70. N. Iwamoto, M. Kamai, and G. Ueno, Examination of Tungsten Carbide Coatings for Thermal Cycling Using NDT, *Thermal Spray: International Advances in Coatings Technology*, C.C. Berndt, Ed., ASM International, 1992, p 405-414
71. L. Giordano, A. Tiziani, A. Zambon, S. Pitteri, and G. Talentino, Comparison between WC-Co Coatings Obtained by APS and CDS on Carbon Steel, *Proc. Second Eur. Conf. Adv. Mater. Processes 1991*, Vol 1, Clyne and Withers, Ed., Institute of Materials, London, 1992, p 307-315
72. C.M. Hackett and G.S. Settles, Turbulent Mixing of the HVOF Thermal Spray and Coating Oxidation, *Thermal Spray Industrial Applications*, C.C. Berndt and S. Sampath, Ed., ASM International, 1994, p 307-312
73. W.D. Swank, J.R. Fincke, D.C. Haggard, and G. Irons, HVOF Gas Flow Field Characteristics, *Thermal Spray Industrial Applications*, C.C. Berndt and S. Sampath, Ed., ASM International, 1994, p 313-318
74. W.D. Swank, J.R. Fincke, D.C. Haggard, G. Irons, and R. Bullock, HVOF Particle Flow Field Characteristics, *Thermal Spray Industrial Applications*, C.C. Berndt and S. Sampath, Ed., ASM International, 1994, p 319-324
75. Y. Wang and P. Kettunen, The Optimization of Spraying Parameters for WC-Co Coatings by Plasma and Detonation-Gun Spraying, *Thermal Spray: International Advances in Coatings Technology*, C.C. Berndt, Ed., ASM International, 1992, p 575-580
76. M.L. Thorpe and H.J. Richter, A Pragmatic Analysis and Comparison of HVOF Processes, *J. Therm. Spray Technol.*, Vol 1 (No. 2), 1992, p 161-170
77. Z.Z. Mutasim, R.W. Smith, and L. Sokol, Vacuum Plasma Spray Deposition of WC-Co, *Thermal Spray Research and Applications*, T.F. Bernecki, Ed., ASM International, 1991, p 165-169
78. G.V. Bobrov, V.B. Shekhov, G.M. Bluykher, and T.E Fomina, Reducing Carbon Losses During the Plasma Torch Spraying of Tungsten Carbides, *Proc. Conf. Poluch. Pokrytii Vysokotemp. Raspylenium*, L.K. Druzhinin, Ed., Atomizdat, Moscow, 1973, p 245-255
79. X. Provot, H. Burlet, M. Vardavoulias, M. Jeandin, C. Richard, J. Lu, and D. Manesse, Comparative Studies of Microstructure, Residual Stress Distributions and Wear Properties for HVOF and APS WC-Co Coatings on Ti6Al4V, *Thermal Spray: Research, Design, and Applications*, C.C. Berndt and T.F. Bernecki, Ed., ASM International, 1993, p 159-166
80. J. Beczkowiak, J. Fischer, and G. Schwier, Cermets for High Velocity Flame Spraying, Publication No. DVS 152, *Proc. Therm. Spray Conf. TS93*, 3-5 March 1993 (Aachen, Germany), Deutsche Verband für Schweisstechnik, Düsseldorf, 1993, p 32-36 (in German)
81. K.S. Zhou, D.J. Yang, A.Q. Zeng, and P.Y. Qi, WC-Cr-Co Coating for Mandrel of Precision Forging Machine, *Thermal Spray: International Advances in Coatings Technology*, C.C. Berndt, Ed., ASM International, 1992, p 393-398
82. L.C. Mei, W.H. Yang, D.M. Du, and L.W. Huang, Characteristics of Two Types of WC-Co Thermal Spraying Powder, *Proc. Int. Conf. Modern Developments in Powder Metallurgy*, Vol 17, 1985, p 251-271
83. C.-J. Li, A. Ohmori, and Y. Harada, Effect of WC Size on the Formation Process of HVOF Sprayed WC-Co Coatings, *Proc. 14th Int. Therm. Spray Conf.*, 22-26 May 1995 (Kobe, Japan), A. Ohmori, Ed., Japan High Temperature Society, 1995, p 869-875